Modulating malignant epithelial tumor cell adhesion, migration and mechanics with nanorod surfaces

**Jiyeon Lee · Byung Hwan Chu · Shamik Sen ·
Anand Gupte · T. J. Chancellor · Chih-Yang Chang ·
Fan Ren · Sanjay Kumar · Tanmay P. Lele**

Abstract The failure of tumor stents used for palliative therapy is due in part to the adhesion of tumor cells to the stent surface. It is therefore desirable to develop approaches to weaken the adhesion of malignant tumor cells to surfaces. We have previously developed SiO_2 coated nanorods that resist the adhesion of normal endothelial cells and fibroblasts. The adhesion mechanisms in malignant tumor cells are significantly altered from normal cells; therefore, it is unclear if nanorods can similarly resist tumor cell adhesion. In this study, we show that the morphology of tumor epithelial cells cultured on nanorods is rounded compared to flat surfaces and associated with decreased cellular stiffness and non-muscle myosin II phosphorylation. Tumor cell viability and proliferation was unchanged on nanorods. Adherent cell numbers were significantly decreased while single tumor cell motility was increased on nanorods compared to flat surfaces. Together, these results suggest that nanorods can be used to weaken malignant tumor cell adhesion, and therefore potentially improve tumor stent performance.

J. Lee · B. H. Chu · T. J. Chancellor · C.-Y. Chang · F. Ren ·
T. P. Lele (✉)
Department of Chemical Engineering, University of Florida,
Gainesville, FL 32611, USA
e-mail: tlele@che.ufl.edu

S. Sen · S. Kumar
Department of Bioengineering, University of California,
Berkeley, CA 94720, USA

A. Gupte
Division of Gastroenterology, Department of Medicine,
University of Florida,
Gainesville, FL 32610, USA

1 Introduction

Tumors that occlude the gastrointestinal, pancreatic and biliary ducts are typically surgically removed, and metallic stents are placed in the ducts for preventing subsequent collapse of the injured tissue (Dormann et al. 2004; McLoughlin and Byrne 2008). However, tumor cell adhesion, migration and proliferation on the installed stents cause stent re-blockage which occurs in 25 to 50% of cases. This requires further surgical interventions for stent removal and causes severe complications in the management of malignancy (Siersema 2008). To overcome such recurrent problems with metallic stents, plastic-covered stents have been developed (Han et al. 2003; Isayama et al. 2002; Togawa et al. 2008). However, plastic-covered stents tend to migrate to other organs (Costamagna et al. 2006; McLoughlin and Byrne 2008) and have poor performance compared to metallic stents (Costamagna et al. 2006; Perdue et al. 2008). Thus, prevention of tumor cell adhesion to the stent surface remains a key challenge (Costamagna et al. 2006; Han et al. 2003; Isayama et al. 2002; Perdue et al. 2008; Siersema 2008; Togawa et al. 2008).

One approach to reduce the blockage of stents is to fabricate nanostructured features on the stent surface that will interfere with tumor cell adhesion. A number of studies have shown that cell adhesion (Arnold et al. 2004; Choi et al. 2007; Milner and Siedlecki 2007), assembly (Karuri et al. 2008), and migration (Yim et al. 2005) are sensitive to the micro- and nano-scale topography of the culture substrate (Balasundaram and Webster

2006; Chun and Webster 2009). These studies have been carried out for cells of non-tumor origin, but there are relatively few studies on tumor cell interactions with nanostructured materials. One study showed that the spreading and proliferation of human osteosarcoma cells decreases on micro-grid titanium coated silicon surfaces with increasing surface roughness (Mwenifumbo et al. 2007). Similarly, the adherent human hepatocellular carcinoma cell number on a silicon nanowire surface was decreased by 60.5% compared to a bare silicon wafer (Qi et al. 2007). We recently reported that coating surfaces with dense monolayers of randomly oriented, upright nanorods significantly reduces adhesion and viability of fibroblasts and endothelial cells (Lee et al. 2009). Cells on nanorods were unable to assemble focal adhesions and stress fibers, which we hypothesized to be due to disruption of integrin clustering on nanorod substrates (Lee et al. 2009). Given that tumor cells have significantly altered adhesive pathways compared to normal cells (Desgrosellier and Cheresh 2010), it is unclear if a similar approach can be used to modulate the adhesion of malignant tumor cells responsible for stent occlusion.

In this paper, we investigated the effect of nanorod coatings on the adhesion, motility, and mechanics of malignant, human esophageal epithelial cells. Malignant tumor cells cultured on nanorod-coated surfaces had significantly decreased non-muscle myosin II activity, decreased stiffness and increased motility. The lack of firm adhesion correlated with an overall decrease in the tumor cell number. Our results suggest that nanorod-based coatings may be a promising approach to decrease tumor adhesion to stent surfaces.

2 Materials and methods

2.1 Growth of nanorods

A solution-based hydrothermal growth method was used for fabricating ZnO nanorods on the substrates (Kang et al. 2007). Briefly, ZnO nanocrystal seed solutions containing 15 mM zinc acetate dihydrate (Sigma Aldrich, St. Louis, MO) and 30 mM of NaOH (Sigma Aldrich, St. Louis, MO) were prepared at 60°C for 2 h and spin-coated onto the substrates. Nanorods were grown by placing seed-coated substrates upside down in an aqueous nutrient solution of 20 mM zinc nitrate hexahydrate and 20 mM hexamethylenetetramine (Sigma Aldrich, St. Louis, MO). A Unaxis 790 plasma enhanced chemical vapor deposition (PECVD) system was used to deposit SiO_2 on the ZnO nanorods at 50°C using N_2O and 2% SiH_4 balanced by nitrogen as reported before (Chu et al. 2008).

2.2 Cell culture

Twenty-two millimeter square glass cover slips (Corning, Inc., Lowell, MA) were used as control substrates. All of the substrates were placed on petri dishes and sterilized with UV for 5 min, and washed with 70% ethanol and de-ionized water. Before cell culture, the substrates were treated with 5 µg/ml human fibronectin (FN) (BD biosciences, Bedford, MA) at 4°C overnight. OE33 (human esophageal epithelial tumor cells) cells were cultured in RPMI supplemented with 10% donor bovine serum (DBS) and 200 mM L-Glutamine (Sigma, St. Louis, MO).

2.3 Cell viability assay

Cells cultured for 24 h on each substrate were stained with the live/dead viability/cytotoxicity kit for mammalian cells (Invitrogen, Eugene, OR) for quantifying adherent cell viability. The number of OE33 cells on glass and nanorods was counted from ten fluorescent images taken randomly using a 20× objective. Three independent experiments of cell viability were performed and the data were pooled. To check for solution toxicity of nanorods, OE33 media was incubated with sterilized nanorods or with glass for 1, 3 and 7 days in an incubator. The conditioned media was next used to culture cells for 24 h. Cell morphology and numbers with nanorod-incubated media was compared to that with glass-incubated media.

2.4 5-bromo-2-deoxyuridine (BrdU) staining

Ten micrometer BrdU (Sigma Aldrich, St. Louis, MO) was added to cells on glass and nanorods (Ammoun et al. 2006). After 20 h of incubation, cells were fixed with 4% paraformaldehyde for 20 min and washed several times with PBS. 2 M HCl was added to the cells and incubated for 20 min at room temperature. Cells were permeabilized with 0.2% Triton X-100 supplemented with bovine serum albumin. Cells were stained with primary anti-BrdU IgG (Sigma Aldrich, St. Louis, MO) and goat anti-mouse secondary antibody conjugated with Alexa Fluor 488 (Invitrogen, Eugene, OR). The number of attached and proliferated cells on glass and nanorods was counted with ten randomly taken images using a 20× objective. Three independent experiments were performed and the data were pooled. A similar fixation and staining protocol was followed for immunostaining of adhesion proteins (Lee et al. 2008, 2009).

2.5 Scanning electron microscopy (SEM)

After 24 h of culture, cells were prepared for SEM by fixation with 2% glutaraldehyde buffered in PBS and post-fixed in 1% osmium tetroxide and dehydrated in graded ethanol concentrations. Critical point drying (CPD) was performed on a Bal-

Tec 030 instrument (ICBR Electron Microscopy Core Lab, University of Florida) and Au/Pd (50 Å) was deposited on the substrate. SEM was performed on a Hitachi S-4000 FE-SEM (ICBR Electron Microscopy Core Lab, University of Florida). Images of samples were taken at 1.0–2.0 k× magnifications.
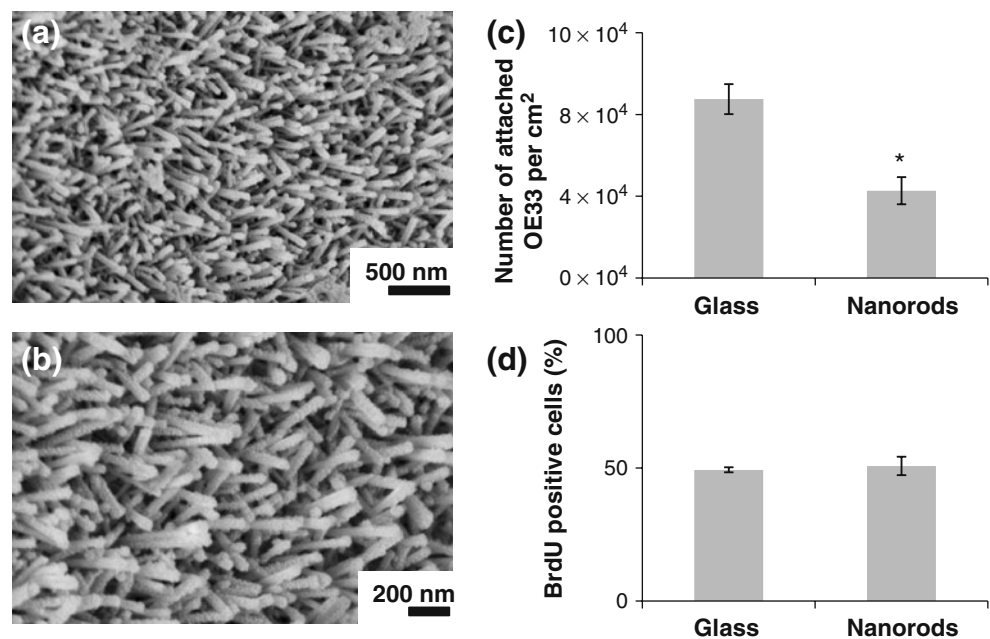
2.6 Cell motility assay

Phase contrast imaging was performed for 12 h on a Nikon TE 2000 microscope with a humidified incubator (*In Vivo* Scientific, St. Louis, MO). Images were collected every 10 min using a 10× objective. The images were then analyzed using a Matlab program that tracked the position of the centroid of cells vs. time. The mean squared displacement was calculated from the data using non-overlapping time intervals (Dickinson and Tranquillo 1993). The speed of each cell was determined from the average displacement in a tracking interval of 10 min. The persistence time of each cell was obtained using nonlinear least-square regression of the mean squared displacement with a persistent random walk model for cell migration as reported elsewhere (Harms et al. 2005).

2.7 Cell stiffness measurement by atomic force microscopy (AFM)

Cells were cultured on FN-coated glass and nanorods for 20 h. An Asylum MFP3D AFM (Asylum Research, CA) coupled to a Nikon TE2000U epifluorescence microscope was used for measuring cell stiffness (Sen and Kumar 2009). The pyramid-tip had a spring constant of 60 pN/nm, and tip half-angle was 37°. One hundred twenty-two cells on glass and 87 cells on nanorods were measured. Each profile was fit with a modified Hertzian model.

2.8 Western blotting

Cells cultured on 76.2 mm × 25.4 mm glass and same size of nanorods were washed with cold PBS and lysed with cell lysis buffer (Cell Signaling Technology, Inc., MA) for 10 min on ice. Cells were then collected and centrifuged at 10,000 rpm for 10 min at 4°C. The supernatant was then collected and SDS-sample buffer was added and stored at −20°C until used. The samples were separated on 10% SDS polyacrylamide gels and then transferred onto a PVDF membrane. The membranes were blocked with 5% milk in TBST at room temperature for 30 min. The membranes were treated with phospho-myosin light chain 2 antibody (Cell Signaling Technology, Inc., MA) at 1:1,000 dilutions in 5% milk overnight at 4°C. The membranes were then washed three times in TBST and treated with peroxidase conjugated secondary antibody at 1:10,000 in 5% milk in TBST for 2 h. Blots were developed using SuperSignal West Pico Chemiluminescent reagent (Pierce Biotechnology, IL) and exposed to X-OMAT film (Eastman Kodak Inc., NY).

3 Results

3.1 Decrease in adhesion of esophageal epithelial tumor cells on nanorods

We used a previously developed method to grow SiO_2 coated nanorods on glass surfaces (Fig. 1(a) and (b)) (Chu et al. 2008). Transmission electron microscopy (TEM) and electrical conductance measurements confirmed that the nanorods were uniformly covered by SiO_2 without any defects (Chu et al. 2008). Nanorod surfaces were then coated with fibronectin

Fig. 1 Esophageal epithelial tumor cell adhesion was decreased on nanorods. (**a**, **b**) SEM images of nanorod morphology. Upright nanorods were covered on the underlying glass substrate uniformly. (**c**) Numbers of attached OE33 cells were reduced by 50% on nanorods compared to the flat glass surface after 24 h culture. (**d**) Cell proliferation is unchanged on nanorods compared to glass as measured by BrdU incorporation. Bars indicate the standard error of the mean (SEM). * indicates statistically significant difference ($p < 0.05$)

Fig. 2 Individual tumor cells in colonies were rounded on nano- rods unlike cells on glass. SEM images of colony on nanorods and glass. Arrows point to lamellipodial structures on glass surface; similar structures were not strongly appeared on nanorods
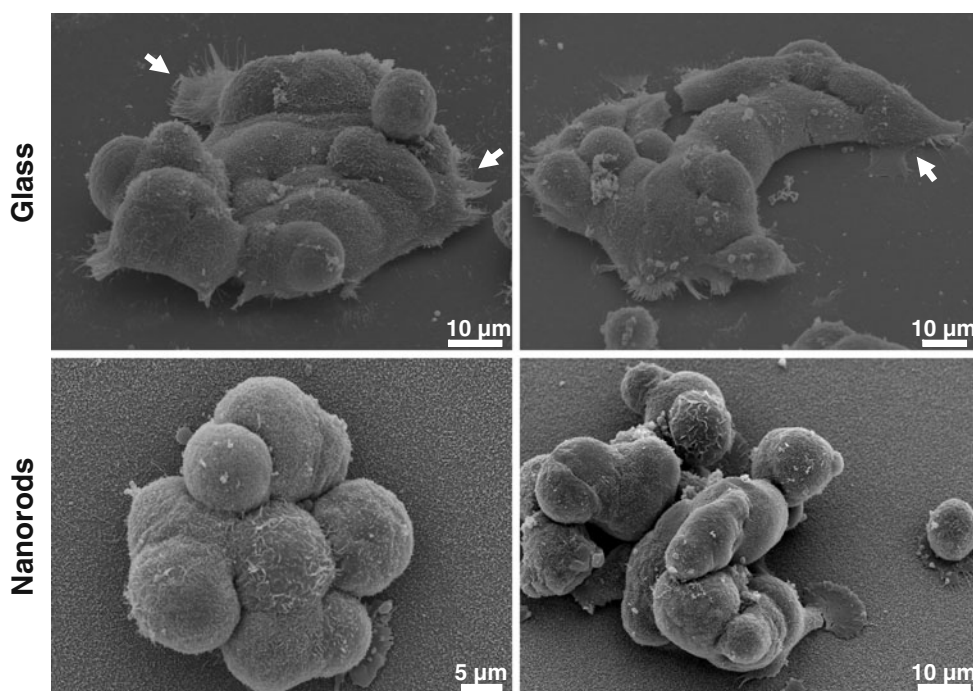
and tumor epithelial cells were cultured on the substrates. After 24 h of culture, the number of adherent tumor cells was observed to be nearly 50% lower on nanorod surfaces compared to glass (Fig. 1(c)). This decrease was not due to toxicity of materials leached from the nanorods themselves (supplementary Fig. 1). We have also previously shown that the SiO$_2$ coated nanorod surfaces are hydrophilic, and fibronectin adsorption is unaltered on these surfaces (Lee et al. 2009). This argues against altered matrix protein adsorp- tion as a potential cause of the decrease in tumor cell numbers.

### 3.2 Viability and proliferation is unchanged in tumor cells on nanorods

Staining with calcein AM (4 μM) and ethidium homodimer-1 (EthD-1) showed that adherent tumor cells on glass and nanorods were both equally viable (data not shown). BrdU staining revealed that tumor cell proliferation on nanorods

was similar to that on glass at 24 h (Fig. 1(d)). Together, these results suggest that the decrease of adherent tumor cells on nanorods is due to weakened adhesion rather than a decrease in proliferation rate or cell viability. The fact the proliferation and viability is unchanged despite weak tumor cell adhesion is consistent with the fact that malignant tumor cells lose their dependence on firm adhesion for survival (Paszek et al. 2005; Tilghman and Parsons 2008).

3.3 Tumor cells cultured on nanorods have decreased contractility

While tumor cells were able to form colonies on nanorods, individual cells in colonies were rounded on nanorods compared to glass (Fig. 2). We next stained cells for vinculin and imaged cells with confocal fluorescence microscopy, but clearly defined focal adhesions proved difficult to detect on both glass and nanorods (supplemen- tary Fig. 2). Cells at the periphery of the colonies were

Fig. 3 Non-muscle myosin II activity is significantly reduced in cells on nanorods compared to cells on glass. Western Blot of phosphorylated myosin shows decreased levels in tumor cells on nanorods. The comparison was made for identical levels of GAPDH to account for the decrease in cell number on nanorods
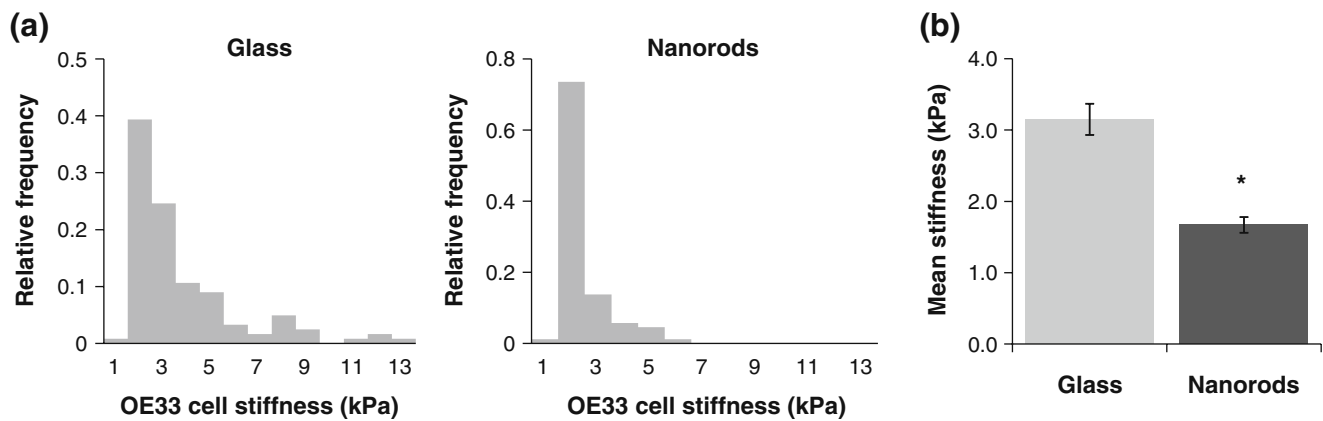
(a)

(b)
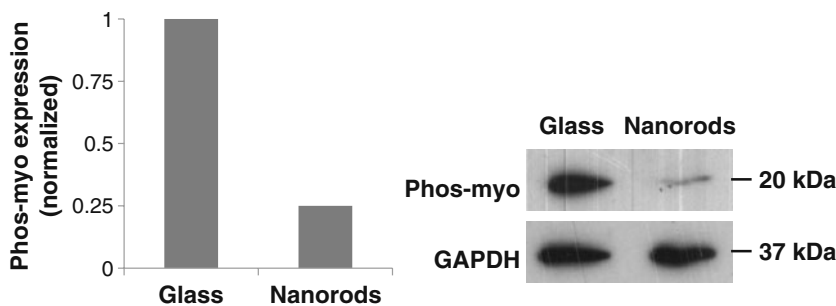
Fig. 4 Tumor cells are softer on nanorods compared to glass. (a) Histograms of single cell stiffnesses measured by AFM on nanorods and glass. (b) The mean cell stiffness on nanorods was decreased by 50% compared to that on glass

observed to form lamellipodial structures on glass (arrows in Fig. 2), but similar structures were less visible on nanorods. These results raised the possibility that nanorods could potentially decrease intracellular tension in the tumor cells.

To evaluate this possibility directly, we next measured the levels of phosphorylated non-muscle myosin II as a measure of intracellular contractility in tumor cells. As seen in Fig. 3, the level of phosphorylated myosin II is significantly decreased in tumor cells adherent to nanorods compared to flat surfaces. These results provide an explanation for the rounded cell morphologies seen in tumor cell colonies on nanorods. It is known that the levels of phosphorylated non-muscle myosin II correlate with the stiffness of the cortical actomyosin cytoskeleton in adherent cells (Clark et al. 2007; Hale et al. 2009). We therefore measured stiffness of the adherent tumor cell cortex using atomic force microscopy (AFM) (Rotsch et al. 1999; Sen et al. 2005). As cell tension is proportional to cortical stiffness (Rotsch et al. 1999), the stiffness can be considered an indirect readout of cell tension. Our measurements revealed that the stiffness of single tumor cells on nanorods was decreased by nearly 50% of that on glass (Fig. 4).

3.4 Single tumor cell motility is increased on nanorods

Cell motility has been previously shown to be sensitive to micro- and nano-scale surface topology (Park et al. 2009; Patel et al. 2010; Thakar et al. 2008; Westcott et al. 2009). For example, fibroblasts migrate faster on surfaces with 500 nm nanoholes compared to the corresponding flat glass surface (Westcott et al. 2009). Similarly, on TiO_2 nanotube surfaces, mesenchymal stem cells and fibroblasts moved faster on 15 nm nanotubes compared with the smooth surface (Park et al. 2007, 2009). However, it is not clear if tumor cell motility is similarly sensitive to nanostructure. We therefore measured the single tumor cell migration speed and persistence time on nanorods. The average cell speed of single tumor cells and the mean persistence time were both found to be increased on nanorods compared with glass (Fig. 5(a) and (b)).

4 Discussion

In this paper, we provide new evidence that actomyosin contractility (as quantified by non-muscle myosin II

Fig. 5 OE33 cell motility is altered on nanorods. (a) The average speed of OE33 on nanorods was higher than that on glass (n=15 for glass, n=16 for nanorods). (b) The mean persistence time is longer on nanorods than on glass (n=9 for glass, n=11 for nanorods). Bars indicate SEM. * indicates a statistically significant difference (p<0.05)

(a)

(b)
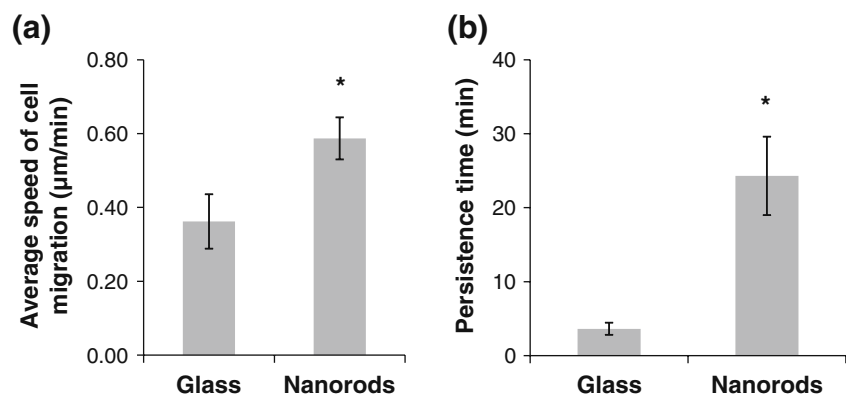
phosphorylation) is decreased in tumor cells on nanorods. Because intracellular tension is balanced by the substrate at adhesive sites, the decrease in myosin activity is expected to correlate with a decrease in cell spreading and adherent cell numbers. Consistent with this, we observed rounded cell morphologies (for both single cells and cells in colonies). We also found a nearly two-fold decrease in the adherent cell number. Interestingly, we observed a decrease in cortical stiffness as measured by AFM, which has been shown to correlate with myosin activity previously (Sen and Kumar 2009). Weakened adhesion may be responsible for the observed increase in motility on nanorods due to easier detachment of the trailing edge of cells (Harms et al. 2005; Palecek et al. 1997). Therefore, our different observations can be explained based on the measured decrease in myosin-based intracellular tension. Additionally, we observed that tumor cell proliferation rate and viability was unchanged on nanorods—this is not surprising given that tumor cells lose their dependence on firm adhesion for survival and proliferation (Paszek et al. 2005; Tilghman and Parsons 2008).

The mechanism of how nanorods alter non-muscle myosin II activity may be (at least in part) due to the nano-scale control of integrin clustering. The clustering of integrins occurs through crosslinking by intracellular proteins like talin (Ye et al. 2010) which causes the formation of stable adhesions that are physically linked to the intracellular actomyosin cytoskeleton. Interfering with integrin clustering interferes with focal adhesion assembly (Arnold et al. 2004; Cavalcanti-Adam et al. 2006, 2007) and feeds back to change actomyosin contractility (Ingber 2006). Work by Spatz and co-workers has shown that integrin clustering requires that adjacent ligated integrin molecules be at a distance of less than 70 nm (Arnold et al. 2004; Cavalcanti-Adam et al. 2006, 2007). Distances higher than these reduce clustering and focal adhesion formation. A similar mechanism may be responsible for our results, although potential intracellular toxicity due to ingestion of nanorods by the cells (Kim et al. 2007) cannot be ruled out.

5 Conclusion

In summary, our results suggest that it is possible to modulate malignant tumor cell adhesion, migration and mechanics with nanorod surfaces. The weakened adhesion raises the possibility that increased tumor cell detachment may occur under shear forces which are commonly encountered in the body (although not studied here). Our results suggest that nanostructure-based approaches may be a powerful yet simple approach to modulate tumor cell

adhesion, which could potentially be used in improving tumor stent performance.

References

S. Ammoun, D. Lindholm, H. Wootz, K.E. Akerman, J.P. Kukkonen, J. Biol. Chem. **281**, 834–842 (2006)

M. Arnold, E.A. Cavalcanti-Adam, R. Glass, J. Blummel, W. Eck, M. Kantlehner, H. Kessler, J.P. Spatz, Chemphyschem **5**, 383–388 (2004)

G. Balasundaram, T.J. Webster, Nanomedicine (Lond) **1**, 169–176 (2006)

E.A. Cavalcanti-Adam, A. Micoulet, J. Blummel, J. Auernheimer, H. Kessler, J.P. Spatz, Eur. J. Cell Biol. **85**, 219–224 (2006)

E.A. Cavalcanti-Adam, T. Volberg, A. Micoulet, H. Kessler, B. Geiger, J.P. Spatz, Biophys. J. **92**, 2964–2974 (2007)

C.H. Choi, S.H. Hagvall, B.M. Wu, J.C. Dunn, R.E. Beygui, C.J.K. CJ, Biomaterials **28**, 1672–1679 (2007)

B.H. Chu, L.C. Leu, C.Y. Chang, F. Lugo, D. Norton, T. Lele, B. Keselowsky, S.J. Pearton, F. Ren, Appl. Phys. Lett. **93**, 233111 (2008)

Y.W. Chun, T.J. Webster, Ann. Biomed. Eng. **37**, 2034–2047 (2009)

K. Clark, M. Langeslag, C.G. Figdor, F.N. van Leeuwen, Trends Cell Biol. **17**, 178–186 (2007)

G. Costamagna, M. Marchese, F. Iacopini, Eur. J. Gastroenterol. Hepatol. **18**, 1177–1180 (2006)

J.S. Desgrosellier, D.A. Cheresh, Nat. Rev. Cancer **10**, 9–22 (2010)

R.B. Dickinson, R.T. Tranquillo, AICHE J. **39**, 1995–2010 (1993)

A. Dormann, S. Meisner, N. Verin, A. Wenk Lang, Endoscopy **36**, 543–550 (2004)

C.M. Hale, S.X. Sun, D. Wirtz, PLoS ONE **4**, e7054 (2009)

Y.M. Han, G.Y. Jin, S.O. Lee, H.S. Kwak, G.H. Chung, J. Vasc. Interv. Radiol. **14**, 1291–1301 (2003)

B.D. Harms, G.M. Bassi, A.R. Horwitz, D.A. Lauffenburger, Biophys. J. **88**, 1479–1488 (2005)

D.E. Ingber, FASEB J. **20**, 811–827 (2006)

H. Isayama, Y. Komatsu, T. Tsujino, H. Yoshida, M. Tada, Y. Shiratori, T. Kawabe, M. Omata, Gastrointest. Endosc. **55**, 366–370 (2002)

B.S. Kang, S.J. Pearton, F. Ren, Appl. Phys. Lett. **90**, 083104 (2007)

N.W. Karuri, P.F. Nealey, C.J. Murphy, R.M. Albrecht, Scanning **30**, 405–413 (2008)

W. Kim, J.K. Ng, M.E. Kunitake, B.R. Conklin, P. Yang, J. Am. Chem. Soc. **129**, 7228–7229 (2007)

J.Y. Lee, B.S. Kang, B. Hicks, T.F. Chancellor, B.H. Chu, H.T. Wang, B.G. Keselowsky, F. Ren, T.P. Lele, Biomaterials **29**, 3743–3749 (2008)

J. Lee, B.H. Chu, K.H. Chen, F. Ren, T.P. Lele, Biomaterials **30**, 4488–4493 (2009)

M.T. McLoughlin, M.F. Byrne, World J. Gastroenterol. **14**, 3798–3803 (2008)

K.R. Milner, C.A. Siedlecki, Int. J. Nanomedicine **2**, 201–211 (2007)

S. Mwenifumbo, M. Li, J. Chen, A. Beye, W. Soboyejo, J. Mater. Sci. Mater. Med. **18**, 9–23 (2007)

S.P. Palecek, J.C. Loftus, M.H. Ginsberg, D.A. Lauffenburger, A.F. Horwitz, Nature **385**, 537–540 (1997)

J. Park, S. Bauer, K. von der Mark, P. Schmuki, Nano Lett. **7**, 1686–1691 (2007)

J. Park, S. Bauer, P. Schmuki, K. von der Mark, Nano Lett. **9**, 3157–3164 (2009)

M.J. Paszek, N. Zahir, K.R. Johnson, J.N. Lakins, G.I. Rozenberg, A. Gefen, C.A. Reinhart-King, S.S. Margulies, M. Dembo, D. Boettiger, D.A. Hammer, V.M. Weaver, Cancer Cell **8**, 241–254 (2005)

A.A. Patel, R.G. Thakar, M. Chown, P. Ayala, T.A. Desai, S. Kumar, Biomed. Microdevices **12**, 287–296 (2010)

D.G. Perdue, M.L. Freeman, J.A. DiSario, D.B. Nelson, M.B. Fennerty, J.G. Lee, C.S. Overby, M.E. Ryan, G.S. Bochna, H.W. Snady, J.P. Moore, J. Clin. Gastroenterol. **42**, 1040–1046 (2008)

S. Qi, C. Yi, W. Chen, C.C. Fong, S.T. Lee, M. Yang, Chembiochem **8**, 1115–1118 (2007)

C. Rotsch, K. Jacobson, M. Radmacher, Proc. Natl Acad. Sci. USA **96**, 921–926 (1999)

S. Sen, S. Kumar, Cell. Mol. Bioeng. **2**, 218–230 (2009)

S. Sen, S. Subramanian, D.E. Discher, Biophys. J. **89**, 3203–3213 (2005)

P.D. Siersema, Nat. Clin. Pract. Gastroenterol. Hepatol. **5**, 142–152 (2008)

R.G. Thakar, M.G. Chown, A. Patel, L. Peng, S. Kumar, T.A. Desai, Small **4**, 1416–1424 (2008)

R.W. Tilghman, J.T. Parsons, Semin. Cancer Biol. **18**, 45–52 (2008)

O. Togawa, T. Kawabe, H. Isayama, Y. Nakai, T. Sasaki, T. Arizumi, S. Matsubara, Y. Ito, N. Yamamoto, N. Sasahira, K. Hirano, T. Tsujino, N. Toda, M. Tada, H. Yoshida, M. Omata, J. Clin. Gastroenterol. **42**, 546–549 (2008)

N.P. Westcott, Y. Lou, J.F. Muth, M.N. Yousaf, Langmuir **25**, 11236–11238 (2009)

F. Ye, G. Hu, D. Taylor, B. Ratnikov, A.A. Bobkov, M.A. McLean, S. G. Sligar, K.A. Taylor, M.H. Ginsberg, J. Cell Biol. **188**, 157–173 (2010)

E.K. Yim, R.M. Reano, S.W. Pang, A.F. Yee, C.S. Chen, K.W. Leong, Biomaterials **26**, 5405–5413 (2005)